Surface plasmons at a metal-insulator interface

Userguide for the Advanced Lab Course

Sebastian Dietl, Leo Prechtel and Markus Mangold

March 31, 2017

In the context of this experiment, the term plasmon denotes a collective, longitudinal excitation of conduction electrons in a metal. More generally, a plasmon is the quantum of a charge carrier density fluctuation in a plasma, a neutral gas of mobile particles which are partly or fully ionized. Following the particle-wave dualism the term plasmon is associated with both quantum of density fluctuation and the wave-like density oscillation. Within the Drude model the conduction electrons in a metal are quasi-free particles which are only slightly damped by the remaining ions and therefore can be treated as a plasma. Note that this would not be valid in the Drude-Lorentz model, since it includes the restoring force created by those ions. When such density oscillations are bound to a metal-insulator interface, they are referred to as surface plasmons (SPs). They go along with a light field coupled to the interface and are therefore also referred to as plasmon-polaritons. In solid-state physics the term polariton accounts for all elementary excitations which couple to light. Surface plasmons have considerable commercial relevance, e.g. in biosensing applications and surface-enhanced Raman spectroscopy (5–8, 11, 19). In addition, SPs attract the attention of contemporary research being touted as an interface between optics and nanoelectronics.
In the *Fortgeschrittenen Praktikum* entitled "Surface plasmons at a metal-insulator interface" a basic understanding of SPs is achieved by determination of the dispersion relation of a surface plasmon at a metal-air interface. The dispersion relation of SPs can be derived from Maxwell's equations. This derivation will be presented in section 1 of this instruction. In the experiment, the reflection of a monochromatic light beam on a thin metal layer is measured as a function of the angle of incidence of the light beam. When the SP is excited, the reflection from the metal layer is attenuated. From the angle, under which the attenuation is strongest, the momentum of the SP at a given energy is determined. In section 2, the experimental setup and the measurement technique are introduced. In section 3 you are given detailed instructions how to measure the SP absorption.

1 Theory

In order to describe the interaction of light with the metal conduction electrons at a metal-insulator interface, we first have to consider the propagation of light in matter as well as on a surface. In section 1.1 the general wave equation for electromagnetic waves in isotropic, homogeneous matter will be derived from Maxwell's equations (10). In section 1.2 we look at the solution of Maxwell's equations at a metal-insulator interface. We find the dispersion relation of a wave propagation at the interface (1, 3, 15). In section 4.2 the derived dispersion relations are discussed. We find that the interface wave is longitudinal, and it is highly localized to the metal-insulator interface. Thus, it is identified as the surface plasmon excitation.

1.1 Electromagnetic waves in matter

Classical electrodynamics is fully described by the set of equations generally known as Maxwell's equations:

$$\nabla \cdot \vec{D} = \rho_{free} \tag{1}$$

$$\nabla \cdot \vec{B} = 0 \tag{2}$$

$$\nabla \times \vec{H} = \vec{j}_{free} + \frac{\partial}{\partial t}\vec{D} \tag{3}$$

$$\nabla \times \vec{E} = -\frac{\partial}{\partial t}\vec{B} \tag{4}$$

Here, $\vec{D} = \epsilon_0\vec{E} + \vec{P} = \epsilon\epsilon_0\vec{E}$ denotes the dielectric displacement field, with $\vec{E}$ and $\vec{P}$ the electric field and the polarization of the medium, respectively, and ϵ the dielectric constant of the medium. $\vec{B} = \mu\mu_0\vec{H}$ is the magnetic flux density with $\vec{H}$ the magnetic field. since we only consider non-magnetic materials with a permeability $\mu \approx 1$ we do not distinguish between $\vec{B}$ and $\vec{H}$. ρ_{free} and $\vec{j}_{free}$ denote free electric charges and current, respectively. We start with a free wave ansatz for the electric and magnetic field to solve the given set of equations, i.e.

$$\vec{E}(\vec{r},t) = \vec{E}_0 e^{-i(\omega t - \vec{k}\vec{r})} \text{ and } \vec{B}(\vec{r},t) = \vec{B}_0 e^{-i(\omega t - \vec{k}\vec{r})} \tag{5}$$

Therein, $\vec{E}_0$ and $\vec{B}_0$ denote the electric and magnetic field amplitude, and ω and $\vec{k}$ stand for the frequency and the wavevector of the alternating fields. Plugged into Maxwell's equations and assuming non-charged materials without free currents / charges,

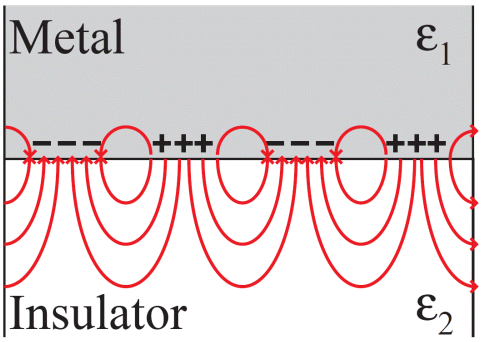

Figure 1: *Sketch of the electrical field distribution of a longitudinal charge carrier oscillation at a metal-insulator interface.*

i.e. $\vec{j}_{free} = \rho_{free} = 0$ this yields

$$\vec{k} \cdot \vec{D} = 0 \tag{6}$$

$$\vec{k} \cdot \vec{B} = 0 \tag{7}$$

$$\vec{k} \times \vec{H} = -\omega \epsilon_0 \epsilon \vec{E} \tag{8}$$

$$\vec{k} \times \vec{E} = \omega \vec{B} \tag{9}$$

Multiplying equation 9 with $\vec{k}\times$ and using equation 6 or 8 we get

$$\vec{k} \times \left(\vec{k} \times \vec{E} \right) = \vec{k} \cdot \left(\vec{k} \cdot \vec{E} \right) - \left(\vec{k} \cdot \vec{k} \right) \cdot \vec{E} = 0 - \left(\vec{k} \cdot \vec{k} \right) \cdot \vec{E} \tag{10}$$

and

$$\vec{k} \times \left(\vec{k} \times \vec{E} \right) = \vec{k} \times \left(\omega \vec{B} \right) = \omega \mu \mu_0 \left(\vec{k} \times \vec{H} \right) = -\omega^2 \mu_0 \mu \epsilon \epsilon_0 \vec{E} \tag{11}$$

Using $\mu = 1$, we derive from the two equations the relation between the wavevector and the frequency of light propagating in a medium, the dispersion relation. In a single particle picture, this is the relation between the momentum and the energy of a photon propagating in a medium:

$$\vec{k} \cdot \vec{k} = \omega^2 \mu \mu_0 \epsilon_0 \epsilon = \left(\frac{\omega}{c} \right)^2 \epsilon \tag{12}$$

This relation is very general and is valid for all electromagnetic waves in a medium (10).

1.2 Electromagnetic waves at a metal-insulator interface

In the following, we want to focus on an electromagnetic wave at a metal-insulator interface. The interface is chosen to lie in the $x - y-$plane at $z = 0$, as shown in figure 1. Additionally, the $x-$axis shall be parallel to the propagation direction of the wave,

such that $k_y = 0$. We start with the ansatz

$$\vec{E}(\vec{r},t) = \begin{cases} (E^0_{x_1}, E^0_{y_1}, E^0_{z_1}) e^{-i(\omega t - (k_{x_1} x + k_{z_1} z))} & z > 0 \\ (E^0_{x_2}, E^0_{y_2}, E^0_{z_2}) e^{-i(\omega t - (k_{x_2} x + k_{z_2} z))} & z < 0 \end{cases} \tag{13}$$

Here and in the following, the index 1 denotes the metallic layer, and the index 2 labels the insulator layer. At the interface, the following boundary conditions have to be fulfilled:

$$\left.\begin{array}{rcl} E_1(\vec{r},t)_x &=& E_2(\vec{r},t)_x \\ E_1(\vec{r},t)_y &=& E_2(\vec{r},t)_y \\ D_1(\vec{r},t)_z &=& D_2(\vec{r},t)_z \\ H_1(\vec{r},t)_x &=& H_2(\vec{r},t)_x \\ H_1(\vec{r},t)_y &=& H_2(\vec{r},t)_y \\ B_1(\vec{r},t)_z &=& B_2(\vec{r},t)_z \end{array}\right\} \text{ for } z = 0 \text{ and arbitrary } x, y. \tag{14}$$

To fulfill the continuity of the x-component of the electric field

$$\vec{E}(\vec{r},t)_x = E^0_x e^{-i(\omega t - (k_{x_1} x + k_{z_1} z))} \tag{15}$$

at $z = 0$ and for all x, we need the x-component of the wavevector to be conserved at the interface, $k_{x_1} = k_{x_2} = k_x$. Furthermore, the x-component of equation 9 together with $H_1(\vec{r},t)_x = H_2(\vec{r},t)_x$ yields

$$\frac{k_{z_1}}{\mu_1} E_y = \frac{k_{z_2}}{\mu_2} E_y \tag{16}$$

Since we assume that $\mu_1 = \mu_2 = 1$ we read from equation 16 that k_z is also conserved at the boundary. This, however, violates the condition in equation 12 which has to be fulfilled for all electromagnetic waves in matter. This contradiction can only be resolved when the $\vec{E}$-field vanishes in y-direction. Thus, from Maxwell's equations it follows that the $\vec{B}$-field and consequently also the $\vec{H}$-field vanishes in x- and z-direction. Our interface wave is a transversal $\vec{H}$-wave, where $\vec{H}$ is perpendicular to the direction of propagation. Its electric and magnetic field are described by the following equations:

$$\left.\begin{array}{l} \vec{E}(\vec{r},t) = (E^0_x, 0, E^0_{z_j}) e^{-i(\omega t - (k_x x + k_{z_j} z))} \\ \vec{B}(\vec{r},t) = (0, B^0_y, 0) e^{-i(\omega t - (k_x x + k_{z_j} z))} \end{array}\right\} \text{with } j = 1, 2 \tag{17}$$

To derive the dispersion relation of the interface wave we exploit the continuity of the z-component of the dielectric displacement field, $\vec{D}_2(\vec{r},t)_z$. Together with $\vec{k} \cdot \vec{D} = 0$ we find that

$$\frac{\epsilon_1}{k_{z_1}} E_x = \frac{\epsilon_2}{k_{z_2}} E_x \tag{18}$$

Additionally we formulate the general dispersion relation of electromagnetic fields in matter, equation 12, for the transversal $\vec{H}$-wave:

$$k_x^2 + k_{z_j}^2 = \frac{\omega^2}{c^2}\epsilon_j, \quad j = 1, 2 \tag{19}$$

Equations 18 and 19 can be transformed into the dispersion relation for the different components of $\vec{k}$:

$$k_{z_j}^2 = \left(\frac{\omega}{c}\right)^2 \left(\frac{\epsilon_j^2}{\epsilon_1 + \epsilon_2}\right) \tag{20}$$

$$k_x^2 = \left(\frac{\omega}{c}\right)^2 \left(\frac{\epsilon_1 \epsilon_2}{\epsilon_1 + \epsilon_2}\right) \tag{21}$$

1.3 Interpretation of the dispersion relations

After the mathematical treatment of the propagation of electromagnetic waves in matter, we examine the physical meaning of the dispersion relations. First, we look at the dispersion of light in a homogeneous material, $\vec{k}^2 = (\frac{\omega}{c})\epsilon$.

- $\epsilon >$ and real. The wavevector $\vec{k}$ is real; an electromagnetic wave can propagate in the medium with the phase velocity $c' = {}^{c}/_{n}$. $n = \sqrt{\epsilon}$ denotes the refractive index of the medium. For $\epsilon =$ const. as it is for many insulators in the visible spectrum, the dispersion relation is a straight line with its slope given by the speed of light in the medium c'.
- $\epsilon < 0$ and real. The wavevector $\vec{k}$ is imaginary; the electromagnetic field decays exponentially on a length scale of ${}^{1}/_{|\vec{k}|}$.
- ϵ complex. The wavevector $\vec{k}$ is complex; an attenuated electromagnetic wave propagates in the medium. It decays on a length scale of ${}^{1}/_{\mathrm{Im}(\vec{k})}$.
- $\epsilon = \infty$. In the artificial case of an electron system without damping the dielectric function has poles. At these frequencies, the system hast a finite response, even in the absence of external forces. The poles of $\epsilon(\omega)$ define the frequencies of free oscillations of the electron system.
- $\epsilon = 0$. From the geometry of longitudinal waves it follows that $\vec{P} = -\epsilon_0 \vec{E}$ or $\vec{D} = \epsilon \vec{E} = 0$. The frequency where the dielectric constant $\epsilon = 0$ is called the plasma frequency. It is the frequency where longitudinal waves in the volume of the metal can exist. Those volume plasma oscillations are not to be confused with surface plasma oscillations, which are the subject of this experiment.

Similar considerations apply for the dispersion of the interface wave. Here, we restrict the discussion to the case of a silver-air interface as it is probably examined in the experiment (gold alternatively). The dielectric constant of silver for a light frequency of $\omega = 3.03 \cdot 10^{15}$ Hz is $\epsilon_{silver} = -15.03 + 1.02i$. The dielectric constant of air is $\epsilon_{air} = 1$.

- the z-component in silver. With the given values, we calculate $k_{z_1} = (0.126 + 4.01i)\frac{\omega}{c}$. The imaginary part of the wavevector is much larger than the real part. The wave is strongly attenuated and will not propagate into the silver bulk.
- The z-component in air. We calculate $k_{z_2} = (0.097 - 0.266i)\frac{\omega}{c}$. Also in air, the wave is strongly attenuated and will not propagate perpendicular to the interface.
- The x-component. We calculate $k_x = (1.03 + 0.0025i)\frac{\omega}{c}$. The real part of the wavevector is much larger than the imaginary part. The wave can propagate for a large distance in x-direction.

We can conclude from the z-component of the wavevector that the interface wave decays quickly with increasing distance from the interface. In other words, the wave is highly localized to the metal-insulator interface. Furthermore, we conclude from $\mathrm{Re}(k_x) >> \mathrm{Im}(k_x)$ that the wave can freely propagate in x-direction. From equation 17 we see that the electric field is polarized in propagation direction of the interface wave. In conclusion, the found solution is a longitudinal surface wave and it is fulfilling all conditions for a surface plasmon. In figure 1 the density oscillations of the conduction electrons due to a surface plasma oscillation is shown schematically. Regions of more positive charge and regions of more negative charge alternate in x-direction. The resulting electromagnetic field is alternating in x-direction and it quickly decays into the bulk of the compositing materials.
So far, we have been talking about electromagnetic waves in matter and on interfaces. However, in quantum mechanics, we have learned about the concept of particle-wave duality. To discuss the interaction of freely propagating light with the surface plasma oscillation it is easier to think in terms of particles. The quantum of propagating light is a a photon. The photon has an energy $E_{photon} = \hbar\omega_{photon}$ and a momentum $p_{photon} = \hbar k_{photon}$. In the former discussion, the dispersion relation gave a relation between the wavevector and the frequency of a wave. In the particles picture, the dispersion relation shows the energy of a particles as a function of its momentum.
The relevant dispersion relations to understand the interaction between a photon and a plasmon are plotted in figure 2. The dashed line represents the dispersion of a surface plasmon at a silver-air interface calculated using equation 21. Under the limit of small wavevectors, the dispersion is approximately linear with its slope equal to the dispersion of light in air, which is indicated by the solid line in figure 2. For larger wavevectors, the dispersion approximates a limiting value determined by the equality $Re(\epsilon_{silver}(\omega)) = -\epsilon_{air}(\omega)$. We see from figure 2 that there is no intersection between the dispersion relations of the plasmon and the photon. However, an intersection indicates a point where the two particles have identical energy and momentum. Since the momentum and the energy have to be conserved when photon and plasmon interact, we learn from figure 2 that no interaction between the plasmon and a photon in air is possible.

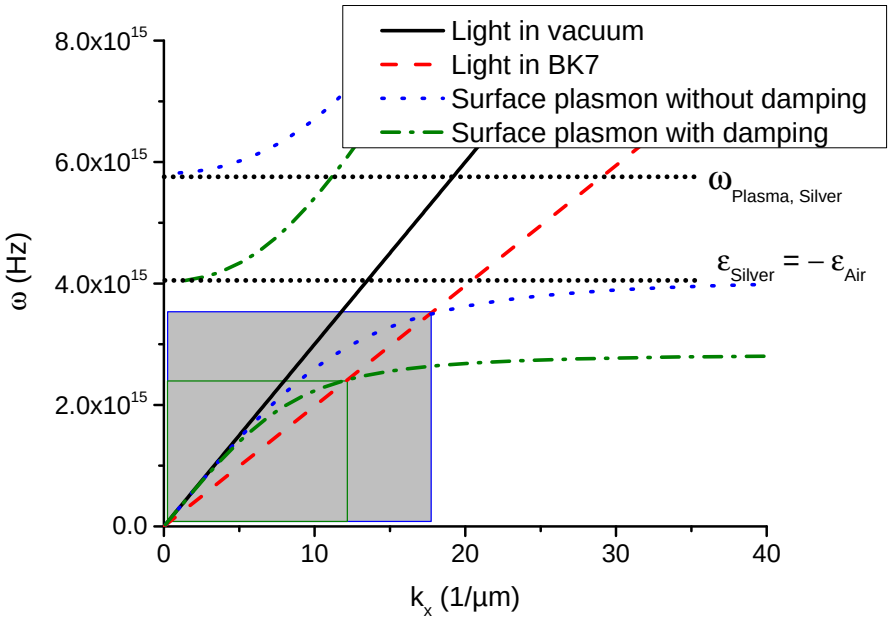

Figure 2: *Calculated dispersion relations of light in vacuum (solid line), light in optical glass BK7 (dashed line), and a surface plasmon with (dash-dotted line) and without damping (dotted line) at a silver-air interface.*

1.4 Otto and Kretschmann configurations

To enable the optical excitation of a surface plasmon, we exploit the reduction of the speed of light in a medium with $\epsilon > 1$. The dispersion of light in such a medium has a smaller slope. In figure 2 the dashed line shows the dispersion of light propagating in optical glass BK7. For a big range of energies the momentum of the photon is larger than the momentum of the plasmon. By changing the angle φ of the incident beam of light we can adjust the x-component of the momentum of the photon to any value $k_{x,photon} \leq \left|\vec{k}_{in}\right|$:

$$k_{x,photon} = \left|\vec{k}_{in}\right| \cdot sin(\varphi) \tag{22}$$

Thus, by choosing the appropriate angle, the surface plasmon can be optically excited in the whole range of frequencies indicated by a gray shade in figure 2. But please note that it is a photon in *glass* which can excite a plasmon at a *metal-air* interface.
Figure 3 shows an experimental configuration enabling the interaction of a photon in glass with a metal-air interface. After its inventor it is named the Otto configuration. The sample consists of a thin layer of air between a glass substrate and a metal layer. The incident light is reflected at the glass-air interface. An exponentially decaying electric field enters the layer of air. The $k_{x,photon}$ component of the wavevector can excite surface plasmons on the metal-air interface. The angle of the incident light φ is changed to match the momentum of the photon to the momentum of the plasmon, $k_{x,photon} = k_{x,plasmon}$.

A different approach utilizes the evanescent field in a thin metal layer. Figure 4

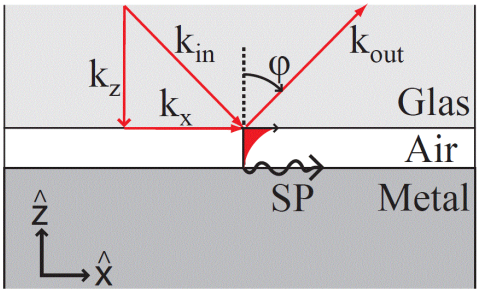

Figure 3: *Optical surface plasmon excitation in the Otto configuration.*

shows the so-called Kretschmann configuration, where a thin layer is prepared on a glass substrate. The incident light is reflected at the glass-metal interface. The $k_{x,photon}$ component of the wavevector of the exponentially decaying light field excites surface plasmons at the metal-air interface. Again, the angle of the incident light φ must be chosen to match the wavevectors of the plasmon and the photon.

When the incident light couples to a surface plasmon, the intensity of the light reflected

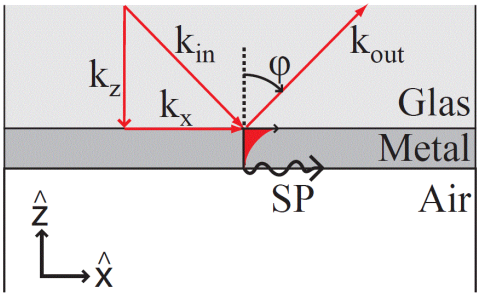

Figure 4: *Optical surface plasmon excitation in the Kretschmann configuration.*

from the metal surface will be reduced. Therefore, in both configurations the intensity of the reflected light is measured as a function of the angle of incidence. A the angle-position of the reflectivity minimum $\varphi_{R_{min}}$ the x-component of the momentum of the incident light $k_{x,photon}$ is matched to the wavevector of the plasmon $k_{x,plasmon}$:

$$k_{x,plasmon} = \left|\vec{k}_{in}\right| \cdot sin(\varphi_{R_min}) \tag{23}$$

In the experiment, we measure $\varphi_{R_{min}}$ as a function of the vacuum wavelength λ_{vac} of the incident light. The wavevector in the glass in related to λ_{vac} by $\left|\vec{k}_{in}\right| = {}^{2\pi}/_{\lambda_{glass}} = {}^{2\pi\sqrt{\epsilon_{glass}}}/_{\lambda_{vac}}$. Equation 23 then becomes

$$k_x = \frac{2 \cdot \pi \sqrt{\epsilon_{glass}}}{\lambda_{vac}} \cdot sin(\varphi_{R_{min}}) \tag{24}$$

Due to the conservation of energy the energy of the surface plasmon $E_{plasmon}$ equals the energy of the exciting photon $E_{photon} = {}^{hc}/_{\lambda_{vac}}$. Thus, by measuring the angle dependent

absorption for different wavelengths one can reconstruct the dispersion relation of the surface plasmon.

2 Experiment

In this experiment you will measure the dispersion relation of surface plasmons at a silver-air or gold-air interface. The Kretschmann configuration will be used to excite the surface plasmons, as it was introduced in section 1.4.
The sample layout and the experimental setup will be described in the following sections. Also, a short introduction to lock-in measurement technique is given.

Q: What are the advantages / disadvantages of both Otto and Kretschmann configuration compared to each other?

2.1 Sample layout

A sketch of the sample layout is given in figure 5. It consists of a BK7 cylinder lens (CL) to which a fused silica cover slip (S) is attached with immersion oil. The index of diffraction for BK7 and fused silica can be found in Appendix 4.2. A thin metal layer is evaporated onto the backside of the cover slip. Ask your advisor for details considering material and layer thickness. The sample can be rotated by an angle φ around an axis Z which is perpendicular to the plane of projection in figure 5. Two micrometer stages (not shown) are used to adjust the position of the axis Z to lie in the center of the cylinder lens under an angle of 90 degree with respect to the surface of the cylinder lens, independent of the angle φ. The light hits the metal layer under the angle φ and is partially reflected under the angle 2φ.

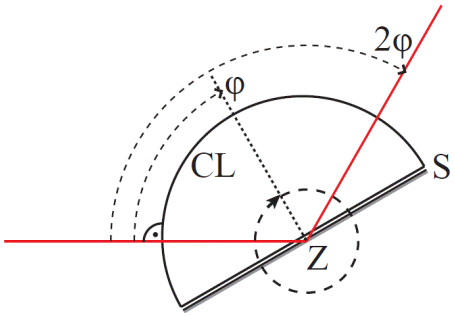

Figure 5: *Sketch of the sample layout. CL denotes the BK7 cylinder lens with the attached sample slip S made of fused silica. Z marks the axis of rotation, oriented perpendicular to the plane of projection.*

Q: Why is it important to have the axis Z lying in the metal layer?
Q: How does the beam path change, if the refractive index of the cylinder lens and the cover slip are different, $n_{CL} \neq n_S$?

2.2 Experimental setup

The experimental setup is shown in figure 6. It consists of a light source (L), a reflector (R), a monochromator (M), an optical chopper (C), a linear polarizing filter (LP), two rotational stages (not shown), and a photodetector (D) which is connected to a lock-in amplifier. The sample is sitting on one rotational stage, the detector is rotated by the second rotational stage. A computer (not shown) is used to operate the rotational stages and to read out the lock-in amplifier.

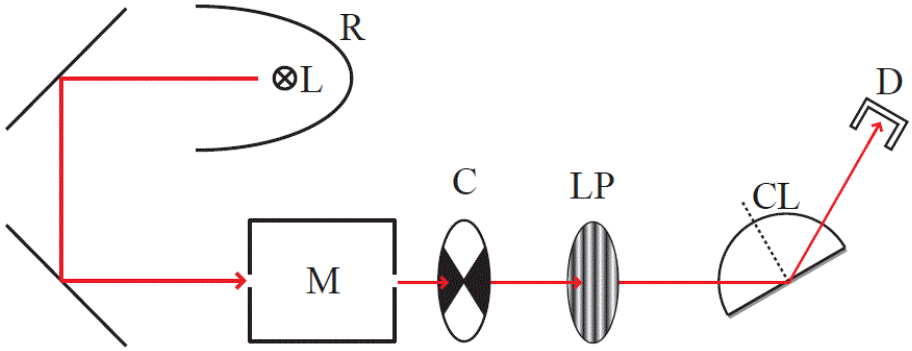

Figure 6: *Schematic view of the experimental setup. Following the light beam, the components are: reflector (R), light source (S), monochromator (M), chopper wheel (C), linear polarizer (LP), cylinder lens (CL) and detector (D).*

Q: Why is a linear polarizing filter LP used? How should the filter be oriented with respect to the rotation axis Z?
Q: What are the advantages of a lock-in amplifier compared with a conventional current-amplifier? What is the purpose of the chopper wheel in this context?

2.2.1 Light source and monochromator

A high-pressure Xenon arc-discharge lamp is used to generate intense light in a spectral range between 350 nm and 1000 nm. The arc is positioned into one focal point of an ellipsoidal reflector. The second focal point of the reflector is guided into the entrance slit of the monochromator. During operation of the lamp there is a DC current of about $3-4$ A at a voltage of about 14 V, resulting in a power of typically ≈ 50 W. To generate the arc, voltage pulses of several kV are applied to the anode / cathode. The xenon lamp generates light from the UV to the far-IR. The spectral emission intensity is strong in the IR and visible range and much weaker for wavelengths closer to the UV. Even though the intensity decreases in the UV, one should not look into the very bright light. In case of lamp failure inform the experiment advisor immediately.
A CARL ZEISS MM 12 double prism monochromator is used to select the desired wavelength in the range from 200 nm and 1000 nm. The optical beam path in the monochromator is shown in figure 7. A display is mounted on the front side of the

monochromator. It shows the selected central wavelength and corresponding wave number, respectively. The spectral width can be tuned by changing the spatial width of the entrance slit and exit slit. A more detailed description of the monochromator can be found in Appendix 4.3.

Q: How does the width of the slit influence the spectral width an intensity of the light beam passing the monochromator? Would it be beneficial for the experiment to adjust the slit very tight or very broad?

2.2.2 Rotational stages and detector

Two rotational stages with coinciding rotation axes are used for rotating the sample and the detector independently. The computer operates both stages, the detector stage is rotated by $2 \cdot \varphi$ and the sample stage by φ. Consequently, the light reflected by the sample is collected by the detector. Unfortunately, the stages can only be rotated relative to an arbitrary initial position. Before starting the measurements, one has to find the positions of the stages corresponding to $\varphi_{sample} = 0$ and $\varphi_{detector} = 0$, which in this case refers to the position where the light beam is parallel to the sample slip and hits the detector. The detector is a preamplified Si-photodiode. It consists of a p-n-junction which is biased with 5 V. Under illumination a photocurrent is induced which is amplified in the preamplifier.

Q: How do you calibrate the positions of the rotational stages? Try to think of a way to do so, which gives the most reliable and reproducible result.

2.3 Lock-In measurement technique

To increase the sensitivity of the photodetector, a lock-in amplification technique is used. In a simplified picture, the lock-in amplifier takes the input signal (voltage), does a Fourier-transformation and filters out all frequency components which are not equal to a certain reference frequency. Thus in order to assign the reference frequency to the signal which should be measured, the light intensity of the beam hitting the sample is modulated by the chopper wheel rotating with the same frequency. The chopper passes the modulation frequency to the lock-in amplifier which uses it as reference.
In a mathematical description, the lock-in amplifier performs a mixing of the input signal S with the modulation signal M. The mixing consists of a multiplication of both signals and a standardized time-integration of the result.
Let us start with the Fourier decomposition of the signal S recorded by the photodetector:

$$S = \sum_i A_i \cdot sin(f_i \cdot t + \Phi_i) \tag{25}$$

Let us assume that the modulation M has the functional form of a sine:

$$M = sin(f_{mod} \cdot t + \Phi') \tag{26}$$

Multiplying S and M and averaging over the time interval T_c yields

$$\frac{1}{T_c}\int_{t=0}^{T_c} SMdt = \frac{1}{T_c}\int_{t=0}^{T_c}\sum_i A_i \cdot sin(f_i \cdot t + \Phi_i)\cdot(f_{mod}\cdot t + \Phi')dt \tag{27}$$

$$\begin{aligned} = \frac{1}{T_c}\int_{t=0}^{T_c}\sum_{i,i\neq mod} &\{A_i \cdot sin(f_i \cdot t + \Phi_i)\cdot sin(f_{mod}\cdot t + \Phi') \\ &+A_{mod}\cdot sin(f_{mod}\cdot t + \Phi_{mod})\cdot sin(f_{mod}\cdot t + \Phi')\}dt \end{aligned} \tag{28}$$

The integration of the first term in 28 will give zero (assuming T_c is chosen to be large enough). Further integration of the second term yields:

$$\begin{aligned} \frac{1}{T_c}\int_{t=0}^{T_c} SMdt = &+\frac{A_{mod}}{2}\cdot cos(\Phi_{mod}-\Phi') \\ &-\frac{A_{mod}}{2f_{mod}T_c}cos(\Phi_{mod}+\Phi'+f_{mod}T_c)\cdot sin(f_{mod}T_c) \end{aligned} \tag{29}$$

The second term in 29 becomes zero for large values of T_c, while the first term does not depend on T_c but on the phase difference $\Phi_{mod} - \Phi'$. Thereby we have show, that the mixing yields the amplitude A_{mod} of the signal S at the modulation frequency f_{mod}, if one choses the modulation phase Φ' appropriately. Experimentally, one sets the phase Φ' at the lock-in amplifier. The amplifier yields the amplitude A_{mod} for the chosen value of Φ' and also the amplitude for the phase shifted by $\pi/2$. Hence, the amplitudes are denoted real part X and imaginary part Y. An equivalent notation can be made using the magnitude M and the phase δ.

Q: What properties must T_c fulfill for the argumentation to be valid?
Q: Calculate the magnitude M and the phase δ from the real and imaginary part X and Y. Do it vice-versa.
Q: Why is a confocal lens pair used to focus the light on the chopper blade?

3 Experimental procedure

Please read the following procedure carefully. If any questions remain, ask your advisors on the day of your experiment.

3.1 Safety instructions

It is essential that you understand the following safety instructions:

- Do not stare into the light! The lamp provides intensive and harmful UV radiation. A safety sheet with documented risks is provided with the experimental setup.
- Do not put anything into the light beam, especially not your skin. Paper will start to burn if you hold it into the white light beam!

- The lamp builds up a high pressure during operation. Even though it is unlikely, the light bulb can explode. The lamp is shielded by the lamp housing. Nevertheless we ask you to leave the lab immediately in case of an explosion.
- The lamp is operated with a high current of several amperes and a voltage of about 15 V. A high voltage of several kV is used to initiate the arc discharge. Therefore, do not alter the electrical wiring of the setup.
- Do not touch anything in this lab besides the setup which will be introduced to you.
- Do not eat or drink in the lab.
- In case of a fire alarm immediately leave the room (do not turn off the lamp or PC). Gather at the meeting point next to the northern Physik II entrance.

3.2 Calibration, parameters and data acquisition

- Optimize the optical pathway for maximum signal detection.
- Ask your advisor for the required *home*-position of sample and detector. Those starting positions will be used as 0 positions in the measurement program of the computer. Try to find a way to calibrate the position of both stages.
- Get acquainted with the lock-in amplifier. Learn how to change the sensitivity and T_c. Use at least $T_c > 20/f_{mod}$ for your measurements. Find the appropriate combination of photocurrent preamplification and sensitivity of the lock-in amplifier. You will have to adjust the sensitivity in every new measurement, the maximum signal amplitude for each measurement should always at least be in the order of 1V.
- A measurement program is used to set the angles φ_{sample} and $\varphi_{detector}$ automatically, to wait for the lock-in amplifier to perform the mixing of the signals, and finally to acquire the amplitude A_{mod} from the lock-in. You have to set the starting angle, the step size and the final angle to perform an angle-resolved reflection spectra.
- The wavelength of the light can be easily changed with the monochromator. The wavelength is shown on the small display on the front of the monochromator. Acquire angle resolved reflection spectra between 950 nm and 450 nm in 50 nm steps. Decrease the wavelength step size to about 25 nm for wavelengths below 450 nm and acquire spectra, until you cannot resolve the position of the reflection dip anymore. Adjust the sensitivity of the lock-in amplifier if the signal amplitude gets too small.
- An important aspect of performing an experiment is writing a documentation of what you did. We therefore ask you to write down any parameter of your measurements and the respective file name in a handwritten lab-book style report. Please hand in a copy of this lab-book with your final report.

3.3 Writing the report

You can fit your acquired data with Mathematica or OriginPro, which are installed on the PC stations in the CIP-pool. Please show your advisers the latest reflection spectra before you leave. The following questions should be answered in the report:

1. Calculate the dispersion relation for surface plasmons from your measured data. Explain how you extract the relevant information from your raw data and provide justification for any approximations you may need.
2. Compare the measured dispersion relation for the surface plasmon with the theoretical prediction. Further detail concerning this task is given in section 4.1.
3. Correct the angle in the experimental dispersion relation for a difference in the diffraction index of the cylinder lens and the cover slip (i.e. BK7 and fused silica glass, see Appendix 4.2. If you find an argument why this angle correction might not be necessary you are allowed to skip it as long as you provide detailed explanation of your thought process.

Please keep in mind that the following scientific standards should be met:

- The report should have a clear structure, beginning with introduction into the experiment, setup, physical background and performance of the experiment. The reader should be able to follow even if he did not perform the experiment himself.
- Graphs need labels at the axes and description of the content. Unlike physical variables, units are not written in italic. You do not need to copy the theoretical derivation of this manual, however each equation which is used in the analysis has to be present. You may copy the figures in this manual.
- Estimate the errors of your measurement.
- Discuss your figures! Compare your results with literature (see section 4.1).
- Give proper citations (Wikipedia is NOT a proper citation).

Please reread your report before handing it in and eliminate any impreciseness in your phrasing. This is an important exercise for future theses.

4 Appendix

4.1 Dielectric function of metals

For comparison of your measured data you can use the database of http://refractiveindex.info, e.g. (2, 12, 16). Please carefully read the abstract/description of the source you are going to cite from, some are more suitable for comparison than others (especially regarding the relative error of the data). Comparison with properties of bulk metals usually gives a very bad agreement with the experiment. Alternatively you can use the Drude model, which gives the dielectric function of a metal as

$$\epsilon_{Metal}(\omega) = 1 - \frac{\omega_{Plasma}^2}{\omega(\omega - i\Gamma)} \tag{30}$$

with ω_{Plasma} the plasma frequency and Γ a phenomenological damping term. You need to find appropriate reference values for those quantities, e.g. (9, 13) (some of those papers calculate in cgs units!). More information, especially about the dielectric function of gold can be found in (4).

4.2 Index of diffraction of BK7 and fused silica

The empirical Sellmeier equation (14) can be used to calculate the effective index of diffraction for a given wavelength:

$$n^2 - 1 = \frac{C_1\lambda^2}{\lambda^2 - C_2} + \frac{C_3\lambda^2}{\lambda^2 - C_4} + \frac{C_5\lambda^2}{\lambda^2 - C_6} \tag{31}$$

Sellmeier coefficients for BK7 and fused silica can be found in table 1.

	BK7	fused silica
C_1	1.03961212	0.6961663
C_2	0.00600069867 μm^2	0.0684043 μm^2
C_3	0.231792344	0.4079426
C_4	0.0200179144 μm^2	0.1162414 μm^2
C_5	1.01046945	0.8974794
C_6	103.560653 μm^2	9.896161 μm^2

Table 1: *Sellmeier coefficients for BK7 and fused silica.*

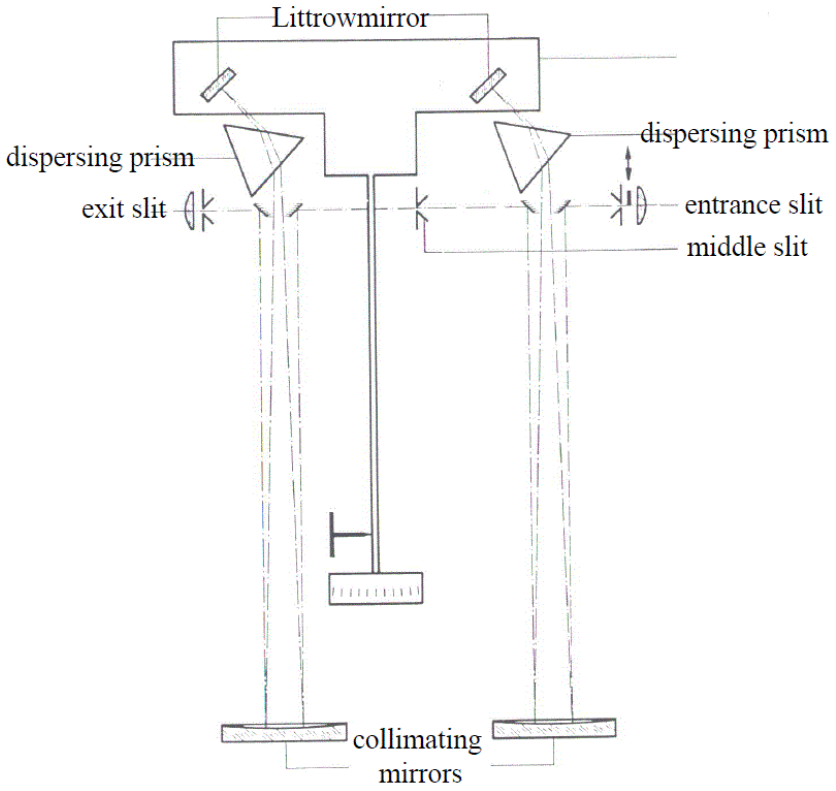

Figure 7: *Optical beam path in the CARL ZEISS MM 12 double prism monochromator.*

4.3 Manual of the monochromator MM 12

The monochromator is model MM 12 Q from CARL ZEISS. Unfortunately the manual can no longer be found online. Thus refer to figure 7 or (17, 18) for the optical beam path in the monochromator and its working principle, respectively.

References

[1] V. M.. Agranovich and D. L. Mills. *Surface Polaritons*. North Holland Publishing Company, Amsterdam and New York and Oxford, 1982.

[2] Shaista Babar and J. H. Weaver. Optical constants of cu, ag, and au revisited. *Applied Optics*, 54(3):477, 2015.

[3] A. D. Boardman. *Electromagnetic Surface Modes*. John Wiley & Sons Ltd., 1982.

[4] P. G. Etchegoin, E. C. Le Ru, and M. Meyer. An analytic model for the optical properties of gold. *The Journal of chemical physics*, 125(16):164705, 2006.

[5] Christy L. Haynes and Richard P. van Duyne. Plasmon-sampled surface-enhanced raman excitation spectroscopy. *The Journal of Physical Chemistry B*, 107(30):7426–7433, 2003.

[6] X. D. Hoa, A. G. Kirk, and M. Tabrizian. Towards integrated and sensitive surface plasmon resonance biosensors: A review of recent progress. *Biosensors and Bioelectronics*, 23(2):151–160, 2007.

[7] Jiří Homola. Present and future of surface plasmon resonance biosensors. *Analytical and Bioanalytical Chemistry*, 377(3):528–539, 2003.

[8] Jiri Homola, Sinclair S. Yee, and Günter Gauglitz. Surface plasmon resonance sensors: review. *Sensors and Actuators B: Chemical*, 54(1–2):3–15, 1999.

[9] P. B. Johnson and R. W. Christy. Optical constants of the noble metals. *Physical Review B*, 6(12):4370–4379, 1972.

[10] Charles Kittel. *Einführung in die Festkörperphyisk*. Oldenbourg, Munich, Wien, 13 edition, 2002.

[11] Jian Feng Li, Yi Fan Huang, Yong Ding, Zhi Lin Yang, Song Bo Li, Xiao Shun Zhou, Feng Ru Fan, Wei Zhang, Zhi You Zhou, De Yin Wu, Bin Ren, Zhong Lin Wang, and Zhong Qun Tian. Shell-isolated nanoparticle-enhanced raman spectroscopy. *Nature*, 464(7287):392–395, 2010.

[12] Kevin M. McPeak, Sriharsha V. Jayanti, Stephan J. P. Kress, Stefan Meyer, Stelio Iotti, Aurelio Rossinelli, and David J. Norris. Plasmonic films can easily be better: Rules and recipes. *ACS photonics*, 2(3):326–333, 2015.

[13] M. A. Ordal, Robert J. Bell, R. W. Alexander, L. L. Long, and M. R. Querry. Optical properties of fourteen metals in the infrared and far infrared: Al, co, cu, au, fe, pb, mo, ni, pd, pt, ag, ti, v, and w. *Applied Optics*, 24(24):4493, 1985.

[14] E. D. Palik. *Handbook of Optical Constants of Solids*. Academic Press, Boston, 1985.

[15] H. Raether. *Surface Plasmons*. Springer-Verlag, Berlin and Heidelberg, 1988.

[16] Aleksandar D. Rakić, Aleksandra B. Djurišić, Jovan M. Elazar, and Marian L. Majewski. Optical properties of metallic films for vertical-cavity optoelectronic devices. *Applied Optics*, 37(22):5271, 1998.

[17] Robert D. Saunders and John B. Shumaker. Apparatus function of a prism-grating double monochromator. *Applied Optics*, 25(20):3710, 1986.

[18] A. Walsh. Multiple monochromators ii application of a double monochromator to infrared spectroscopy. *Journal of the Optical Society of America*, 42(2):96, 1952.

[19] Hongxing Xu, Erik J. Bjerneld, Mikael Käll, and Lars Börjesson. Spectroscopy of single hemoglobin molecules by surface enhanced raman scattering. *Physical Review Letters*, 83(21):4357–4360, 1999.